Available online at www.sciencedirect.com
ScienceDirect
Acta Materialia 57 (2009) 4036–4045
Acta MATERIALIA
www.elsevier.com/locate/actamat

Simulations of hydrogen diffusion at grain boundaries in aluminum

Andreas Pedersen *, Hannes Jónsson

Faculty of Science and Science Institute, University of Iceland, Dunhaga 3, 107 Reykjavík, Iceland

Received 15 January 2009; received in revised form 24 April 2009; accepted 26 April 2009
Available online 6 June 2009

Abstract

Long-timescale simulations of hydrogen atom diffusion in aluminum at low concentration were carried out to study the effect grain boundaries can have on the diffusion mechanism and diffusion rate. Three different grain boundaries were studied: Σ5 twist, Σ5 tilt and general, twist + tilt, grain boundaries. The adaptive kinetic Monte Carlo method was used to simulate the system over time intervals spanning tens of microseconds. A potential function of the effective medium form was parametrized to density functional theory calculations and used to describe the atomic interactions. The twist boundary turns out to block diffusion across the boundary – only a few high-energy sites are found in the boundary layer. However, diffusion parallel to the boundary is slightly enhanced because of the reduced configuration space. The twist and twist + tilt grain boundaries have strong binding sites within the boundary layer, up to 0.1 and 0.3 eV stronger, respectively, than binding sites in the crystal. In the latter case, the H atom spends more than 99% of the time in the grain boundary layer and diffusion parallel to the grain boundary occurs only when the H atom re-enters a crystal grain. Because of the trapping, the diffusion is reduced by more than an order of magnitude compared with the crystal.

Keywords: Grain boundary; Hydrogen diffusion; Adaptive kinetic Monte Carlo; Long-timescale

1. Introduction

Structural defects in crystals, such as grain boundaries (GBs), have an important effect on the physical and chemical properties of materials and are particularly important in materials consisting of nanosized grains. In particular, the absorption and diffusion of hydrogen in metals is expected to be strongly affected by crystal defects. These effects are difficult to measure directly, but some experimental work has been carried out to address this and related issues. It is generally agreed that solubility of hydrogen is increased when GBs are introduced. This has been measured, for example, in aluminum by Edwards and Eichenauer [1], who observed decreased solubility as crystalline grains increased in size from 1 to 5 mm. Mütschele and Kirchheim [2] also found that the GB region offers strong binding sites for H atoms and suggested that the hydrogen solubility of a sample can be used to probe the abundance of GBs in the sample. Others have emphasized the importance of other types of defect sites for hydrogen absorption, such as dislocations and vacancies [3].

The effect of GBs on hydrogen diffusion is less well understood. From their experimental results, Mütschele and Kirchheim [4] concluded that the diffusion coefficient depends on the hydrogen concentration. At low concentrations, where H–H interactions can be neglected, GBs impede diffusion, whereas at high concentrations the GBs provide a fast pathway for diffusion. This could explain why GBs have in one case been observed to create a 40-fold increase in diffusivity [5] and in another case, where the hydrogen content was low, they caused a reduction in diffusivity [6]. For hydrogen diffusion in aluminum, experiments by Ichimura et al. [7] show a non-monotonic dependence of the diffusivity on grain size: as the grains were made smaller, a slight increase in diffusivity was observed for large, columnar grains, but then a sharp decrease in diffusivity followed as the grains were made even smaller.

On the theoretical side, there has not been much effort made to address these issues. The problem is that the

* Corresponding author. Tel.: +354 8688177.
E-mail address: andreas@theochem.org (A. Pedersen).

1359-6454/$36.00 © 2009 Acta Materialia Inc. Published by Elsevier Ltd. All rights reserved.
doi:10.1016/j.actamat.2009.04.057

simulated systems need to be large and the calculations of hydrogen binding and diffusion need to sample a complex energy landscape. Szpunar et al. [8] simulated the classical dynamics of a hydrogen atom in the vicinity of twin–twist GBs in nickel. From an analysis of the mean squared displacement, they concluded that the diffusivity is enhanced at these GBs.

We report here on long-timescale simulations of a hydrogen atom in the vicinity of three different GBs in aluminum and evaluate the binding energy at different sites, as well as the diffusivity parallel and perpendicular to the GBs. The simulation method is described in the next section, then the simulated systems and finally the simulation results.

2. The simulation methods

2.1. Long-time dynamics

In order to be able to simulate the system on a timescale that is long enough to identify diffusion paths and evaluate diffusion constant, we have used the adaptive kinetic Monte Carlo (AKMC) method [9]. This method has previously been applied to several materials related studies, in particular surface diffusion and crystal growth [10]. The method is based on the harmonic approximation to transition state theory (HTST), where the rates of various thermally activated processes that can occur in the system can be estimated from

$$k_j^{\mathrm{HTST}} = \nu_j \exp\left[-\frac{E_{\mathrm{SP},j} - E_R}{k_B T}\right] \tag{1}$$

$$\nu_j = \frac{\prod_i^D \nu_{R,i}}{\prod_i^{D-1} \nu_{\mathrm{SP},j,i}} \tag{2}$$

Here E_R is the energy of the initial state of the system, $E_{\mathrm{SP},j}$ is the energy of the saddle point (SP) associated with the transition mechanism j, and the prefactor ν_j is the ratio of the product of vibrational frequencies in the reactant state, $\nu_{R,i}$, and at SP $\nu_{\mathrm{SP},j,i}$. Note, that the unstable mode, corresponding to a negative eigenvalue at the first-order SP, is not included, so the number of vibrational modes at the SP is one less than at the minimum. Physically, ν_j can be thought of as the attempt frequency for the specific mechanism.

The most challenging task in the application of HTST and Eq. (1) is the identification of all the relevant SPs on the potential energy rim surrounding the given initial state. In the AKMC method, the minimum-mode-following method is applied to climb up from the initial state minimum to an SP without any preconceived notion of the mechanism of the transition or the final state. This is repeated several times, starting from different random displacements, in order to get a sampling of the SPs. The climb is carried out by reversing the force component parallel to the eigenmode of the mass-weighted Hessian that corresponds to the smallest eigenvalue – the "minimum-mode". Determining the eigenmodes of the Hessian is a computationally intensive task for large systems, but since only the lowest eigenmode is needed this can be avoided and only the minimum-mode need be estimated directly with the dimer method [11].

A key feature of the AKMC method is that the table of possible events that can take place in the system is constructed during the simulation for each visited site. This distinguishes the method from the ordinary kinetic Monte Carlo method, where the table of events is constructed before the simulation starts and is therefore based on a preconceived notion of the transition mechanism and rates. An important aspect of the AKMC method is the need to carry out sufficiently many SP searches from sufficiently different initial conditions to get a thorough enough sampling of the relevant SPs. The choice of parameters for efficient sampling has been discussed in previous publications [9,12]. The first step in a climb up to an SP involves displacement of some of the atoms in the system. In the present case, all atoms within a spherical region of radius 3.5 Å centered on the hydrogen atom are displaced using random numbers in such a way that the length of the displacement vector is normalized to 1 Å. The minimum-mode method is then used to climb up the energy surface and converge on a saddle point. A, SP search is considered converged when the norm of the force vector drops below 25 meV $\mathrm{Å}^{-1}$. Searches are carried out until 50 of them have converged on saddle points that connect with a minimum energy path to the given initial state.This criterion was tested on a few initial states by performing 1000 converged SP searches. The number of searches that converged to the lowest energy process was well above 8% and 50 searches were found to include the most significant transition mechanisms.

When the adapted table of events is considered complete an event is picked from the table according to the relative transition rates using a random number. The time interval in the evolution of the system the event represents is estimated as

$$\Delta t = \frac{-\ln \mu}{\sum_j k_j^{\mathrm{HTST}}} \tag{3}$$

where μ is a random number between zero and one and j runs over all the events in the table. After a transition mechanism has been chosen and a time step determined, the system is brought to the corresponding final state. An iteration has then been completed and the SP searches for the next state are carried out.

When determining the prefactor, ν, an approximate Hessian is used as only the atoms that are displaced by more than 0.25 Å during the process and the neighbors within a radius of 3.5 Å are then included in the eigenvalue problem. Other atoms are kept froze when the Hessian matrix is constructed.

2.2. Atomic interactions

Information about the interaction of hydrogen with aluminum can be obtained from previous experimental measurements and theoretical calculations. For aluminum

Table 1
Parameters for Al and H in the EMT potential function, in units derived from eV and Å.

	E_0	V_0	n_0	s_0	η_2	λ	κ
Al	−3.280	1.493	0.047	1.588	2.343	2.209	2.343
H	0.784	2.398	0.182	0.530	4.401	2.398	4.457

The parameters are as defined in Ref. [15].

Table 2
Target values in the fit of the EMT potential parameters.

	Tetrahedral site (eV)	Octahedral site (eV)	Saddle point (eV)
DFT	0.0 (0.69)	0.13	0.18
EMT	0.0	0.1297	0.1762

The values are relative to the hydrogen embedding energy at a tetrahedral site (given in parenthesis). The DFT values are from Ref. [14], Fig. 8.

crystal it is experimentally observed that the solubility of hydrogen is well below an H/Al atomic ratio of 10^{-10} when extrapolated to room temperature [13]. The interstitial diffusivity at ambient temperature and pressure is reported to be 10^{-11} (m^2 s^{-1}) [3]. Density functional theory (DFT) calculations by Wolverton et al. [14] give an energy of 0.69 eV for a hydrogen atom at the interstitial tetrahedral site in an Al crystal compared with binding in a hydrogen molecule. Binding at an octahedral site is even higher in energy, 0.82 eV. The minimum energy path for a hydrogen atom to diffuse in the aluminum crystal has a saddle point that is 0.18 eV above the energy of the tetrahedral site. The activation energy of diffusion is, therefore, estimated to be 0.18 eV within HTST.

To model the atomic interaction in the present study, an effective medium theory (EMT) potential function was used [15,16]. The potential parameters were selected to fit the DFT calculations (see Tables 1 and 2). One should note that this potential function should be used with care as the fit was done towards such a small set of target values. The implementation of the potential function in Asap[1] was used.

2.3. EON2

The simulations were done using the EON2[2] software, which is freely available to carry out AKMC calculations in a distributed manner. With this, advantage is taken of the fact that the SP searches are independent and multiple searches can be carried out simultaneously on different computers that are connected via the internet. EON2 uses BOINC[3] as the communication framework for a server/client approach.

The key parameters for the AKMC simulations as described in Section 2.1 are restated and listed in Table 3.

Table 3
AKMC parameters for the long-timescale simulations.

	Server side	Client side
Temperature	300 K	
Near saddle points	50	
Initial displacement, saddle point		1 Å
Converged, saddle point		25 meV $Å^{-1}$
Minimum movement, prefactor		0.25 Å
Moved within radius, prefactor		3.5 Å

All parameters are described in Section 2.1.

3. The simulated systems

Four different systems were simulated to gain an insight into the H atom diffusion in Al. As a reference system, a perfect Al crystal containing one H atom was simulated. Furthermore, three different GBs were simulated, two high-order Σ5 GBs being either twisted or tilted and one general boundary being both twisted and tilted. When simulating the perfect crystal all atoms were free to move and periodic boundary conditions were applied in all directions. For the GBs, the Z-direction was not subject to periodic boundary conditions; rather, the atoms in the two outermost layers were kept fixed to minimize surface effects. The structural data are summarized in Table 4. The atomic structure of GBs is not well known and the generation of such structures is a non-trivial task. Here, the following scheme was used: for the twist GB, the two single-crystalline grains were rotated with respect to each other (36.9°) and their [100] surfaces were brought into contact. The γ-surface for this structure was mapped out and the grains were accordingly slid in the X–Y-plane to minimize the energy. The structure was then annealed for 125 ps at an elevated temperature using a classical dynamics simulation with a Langevin thermostat. At the end of each 5 ps period a sample was recorded and energy minimized. Among these 25 minimized configurations, the one with the smallest energy was chosen for the diffusion simulation. As a final adjustment before the diffusion simulation, the strain in the Z-direction was relieved. This was done to minimize the influence of the outermost fixed layers. The Z-coordinates were scaled to get a minimum in the energy. For the tilt GB, a similar procedure was followed, but it should be noted that during the annealing the GB moved upward into the upper grain, as is illustrated from the color-coding of atoms in Fig. 4.

Table 4
The four simulated systems.

	Crystal	Twist GB	Tilt GB	Twist + tilt GB
Periodicity	XYZ	XY	XY	XY
Al atoms	256	900	850	1094
Free atoms	256 (+1)	700 (+1)	680 (+1)	908 (+1)

All structures contain a H atom in addition to the Al atoms, thus the (+1) in the row for free atoms.

[1] http://wiki.fysik.dtu.dk/asap/
[2] http://theochem.org/~andreas/programming.html
[3] http://boinc.berkeley.edu

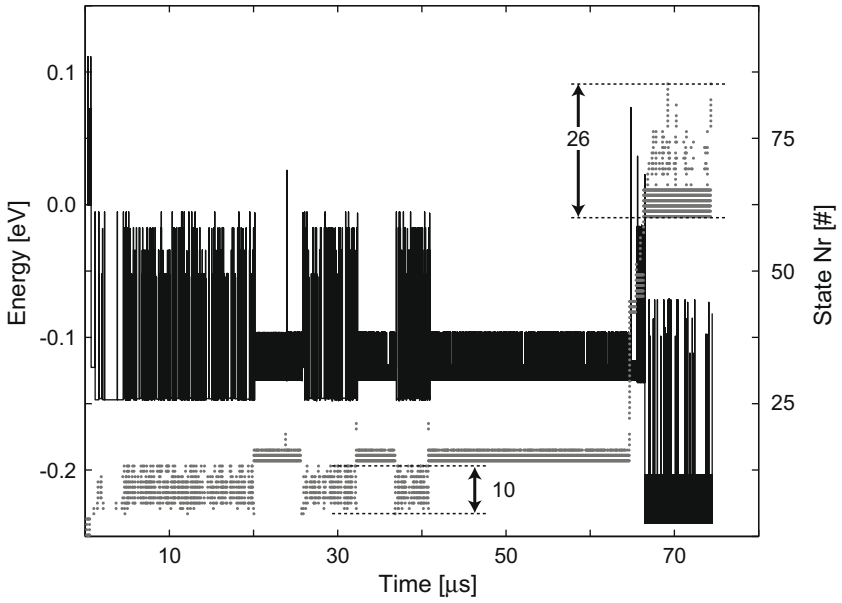

Fig. 1. Long-timescale annealing of the Al twist + tilt GB before the H atom is introduced. The simulated time spans a period of 74 μs. The energy of the system is lowered by 0.24 eV during the annealing, mainly due to two distinct annealing events. During the simulation, two basins of low-energy configurations are visited that consist of 10 and 26 configurations. The lowest energy configuration is then used for the H atom diffusion simulation.

The general, twist + tilt GB was based on the lowest energy configuration from an earlier simulation of such a GB in Cu [17]. This configuration was rescaled to fit the lattice constant of aluminum and long-timescale AKMC simulations were carried out to anneal the sample before introducing the H atom. The annealing temperature was 300 K and the time interval spanned 75 μs. During this time interval a lowering of 0.24 eV was obtained and 86 unique states were visited, as can be seen in Fig. 1. From the figure it appears that two basins of low-energy configurations were visited where the first consists of 10 and the second of at least 26 configurations. Among the latter group is the lowest energy configuration found, and this was used for the H atom diffusion simulation. The mechanism that brought the system into the second basin is shown in Fig. 2 and involved as many as 11 atoms being displaced more than 0.5 Å; however, the barrier that the system had to overcome was only 10 meV.

4. Results

After preparing the structures as described in Section 3 the long-timescale simulations of hydrogen atom diffusion were started. The total time simulated and the number of transitions and unique states visited are listed in Table 5. It should be noted that the total time simulated for the

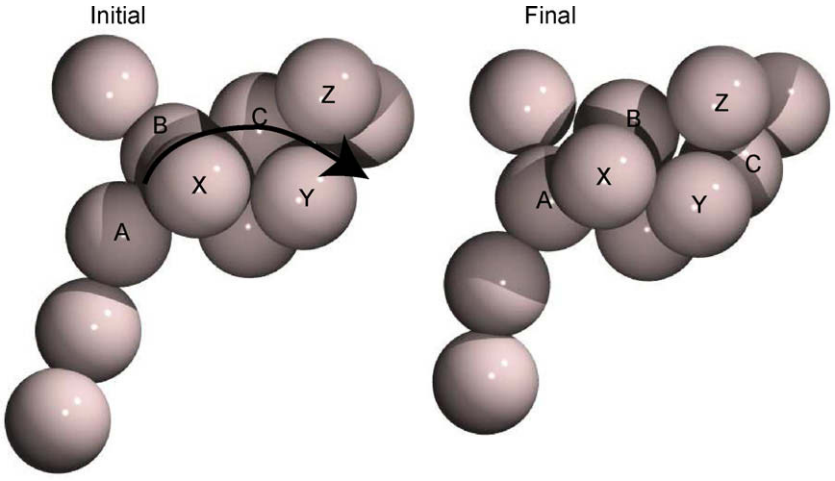

Fig. 2. Annealing event that brings the Al twist + tilt GB into the final, lowest energy basin as seen in Fig. 1. A total of 11 atoms are displaced more than 0.5 Å and are the ones displayed in the figure.The labelled atoms define the core of the displacement. A, B and C can be assigned to the lower grain, and X, Y, Z to the upper grain. The barrier for the transition is only 10 meV.

Table 5
Some statistics on the four diffusion simulations.

	Crystal	Twist GB	Tilt GB	Twist + tilt GB
Time simulated	138 ns	101 ns	101 ns	9.6 μs
Transitions	3195	3352	9774	1.09×10^6
Unique states	1043	975	1185	3417

twist + tilt GB is approximately two orders magnitude larger than for the other GBs and for the crystal, whereas the ratio of unique states visited is only 3.5. The diffusion paths for the H atom in the vicinity of the different GBs are shown in Figs. 3–5. In the last case, the GB region is broader and harder to identify. Here, common neighbor analysis was used to classify the local environment of each atom and to identify those that are in a face-centered cubic (fcc) crystal environment and those that are in the GB [18].

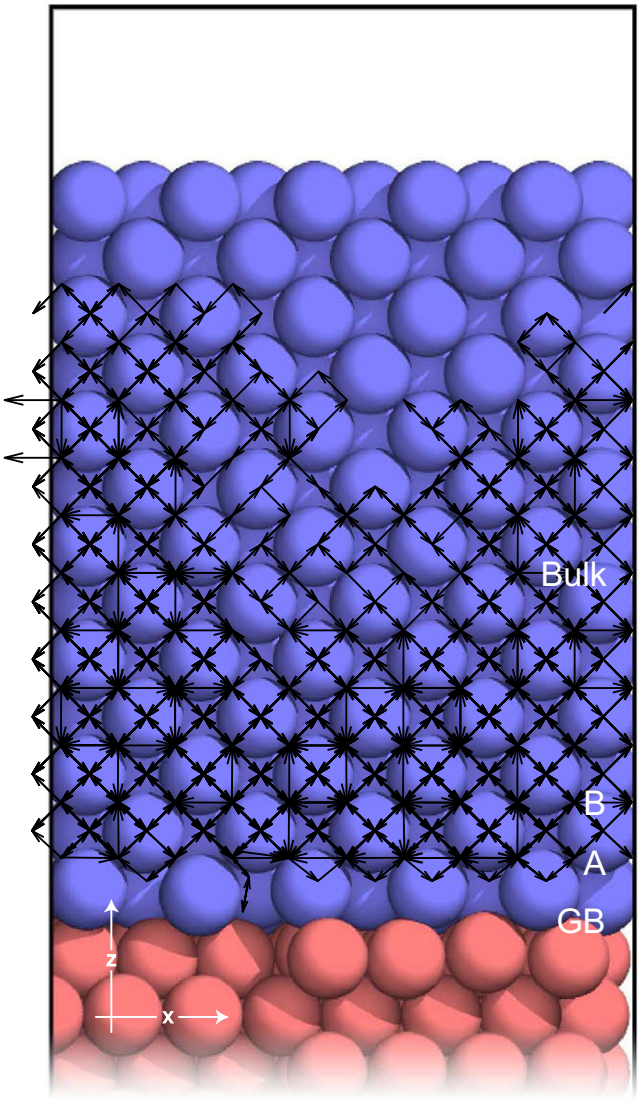

Fig. 3. H atom diffusion path at the vicinity of a Σ5 twist GB projected onto a representative plane of the GB structure. The H atom does not cross the grain boundary plane. Atoms belonging to the upper grain are colored blue, while the atoms in the lower grain are red. (For interpretation of the references to color in this figure legend, the reader is referred to the web version of this article.)

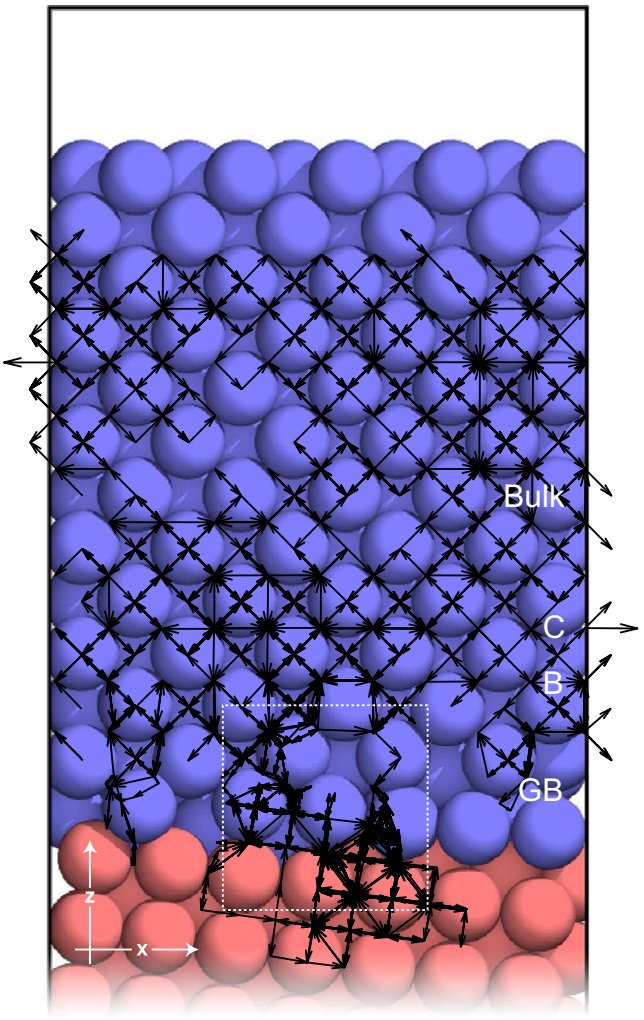

Fig. 4. H atom diffusion path at the vicinity of a Σ5 tilt GB projected onto a representative plane of the GB structure. Unlike the twist GB, the H atom can cross the tilt GB, but only in the limited region marked by the dashed white square. The square also identifies the region of the PES shown in Fig. 9. Atoms initially belonging to the upper grain are colored blue, red is used for the lower grain. One should note that the GB layer has moved upward into the upper grain. (For interpretation of the references to color in this figure legend, the reader is referred to the web version of this article.)

From the diffusion path in the vicinity of the twist GB it is evident that the H atom stays in the upper grain and that the GB is never crossed. For both the tilt and twist + tilt GBs, the H atom crosses the GB. In the case of the tilt GB, there is a distinct channel for the perpendicular diffusion. For the twist + tilt GB, the path reveals that the density of stable sites for the H atom within the GB is higher than in the crystal grains.

During the simulation of the diffusion at the tilt GB an annealing event took place after about 250 iterations. This is shown in Fig. 6. The energy of the system was lowered by 0.06 eV by this event, as is evident from the figure, where the energy of tetrahedral (0.0–0.06) eV and octahedral sites

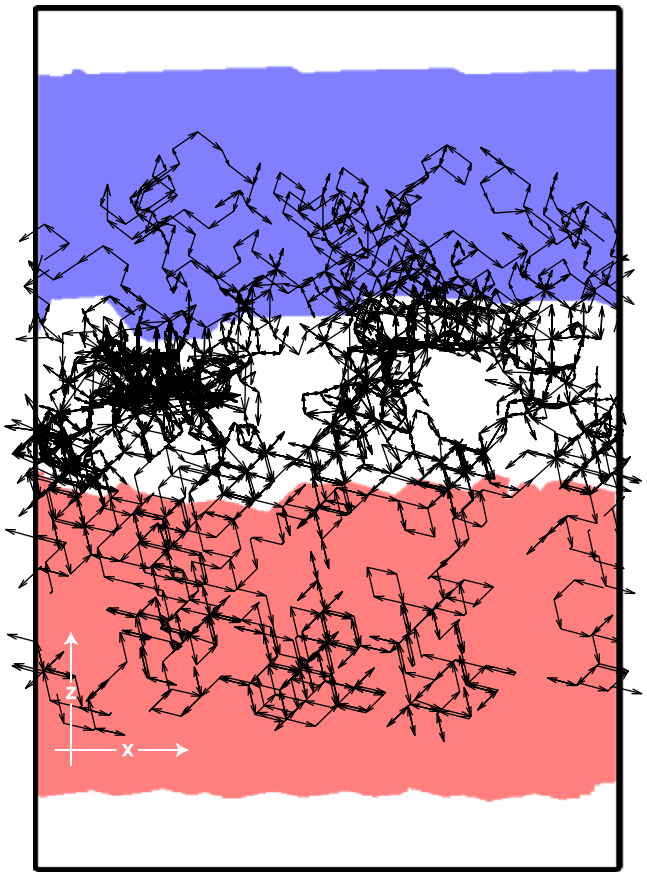

Fig. 5. H atom diffusion path projected onto a schematic of the twist + tilt GB structure. In the schematic the GB region is not colored (defined as atoms not being fcc-coordinated; see Ref. [18]), the region of fcc-coordinated atoms in the lower grain is shown in red and the region of fcc atoms in the upper grain is shown in blue. Within the GB region the density of low-energy sites is high. (For interpretation of the references to color in this figure legend, the reader is referred to the web version of this article.)

(0.22–0.28) eV both are shifted by 0.06 eV towards lower energy.

5. Analysis

To determine the diffusion constant at room temperature from the obtained data, the Einstein–Smoluchowski equation for a random walk is applied:

$$D = \frac{\langle |\mathbf{r}(t+\tau) - \mathbf{r}(t)|^2 \rangle}{2d\tau} \quad (4)$$

where d is the dimensionality of the system and has been set to two as the H atom is confined to two dimensions by the frozen layers, which act as reflecting walls. The calculated diffusivity of a H atom in a slab without a GB was determined for comparison. In the analysis of these simulations, the dimensionality parameter, d, is set to two. Note that the same value of the diffusivity is obtained from simulations of diffusion in the perfect, 3D crystal, and a value of $d = 3$ is used. This value of the diffusivity is within an order of magnitude of the reported experimental value for interstitial H in pure Al [3]. The diffusivity parallel to the GB determined from the simulations is summarized in Table 6 and shown in Fig. 7. To gain an understanding of the different parallel diffusivity for the three GBs, an analysis of the energy landscape for the H atom was carried out. For the twist and tilt GB the minimum energy path was calculated for certain parts of the structures, whereas the analysis of the twist + tilt GB was based on the energy of the stable states visited during the simulation.

5.1. Twist grain boundary

The minimum energy path for an H atom approaching the twist GB along the Z-direction is shown in Fig. 8. It shows clearly why the trajectory in Fig. 3 never crosses the GB. From the B-layer and inwards to the GB layer the energy increases significantly, causing the effective barrier for an H atom to enter a stable site within the GB to be 0.45 eV. A diffusion hop in the crystal at room temperature is roughly 5×10^4 more probable than entering the GB. Within the GB itself, the density of the stable states is low since the sites are all high in energy and it is highly improbable that H atom diffusion would take place there. The parallel diffusivity is found to be slightly larger near a twist GB than within a perfect crystal. The minimum energy path for parallel diffusion close to the GB does not show any distinct features; rather, it is very similar to diffusion in the crystal. The twist GB only affects the energetics in the close vicinity of the GB. A very slight decrease in energy is found in the second layer, labelled B in Fig. 3, and that may contribute to the observed increase in the parallel diffusivity.

5.2. Tilt grain boundary

The diffusivity parallel to the tilt GB is half the value for a perfect crystal. The irregularities of the structure makes it problematic to perform a consistent analysis of minimum energy paths. In the following analysis this is overcome by constructing a potential energy surface (PES) as a projection of the lowest energy states in a selected region of the X–Z-plane. The PES and the H atom's trajectory are shown in Fig. 9. Two low-energy basins are evident from this figure. They form the two channels connecting the upper and lower grains, as observed in Fig. 4. From the PES it can also be seen that the tilt GB has some high-energy sites analogous to the twist GB. The minimum energy paths for parallel diffusion are shown in Fig. 10. The plot shows that the influence of the tilt GB on the energy is larger than for the twist GB, although already in the C-layer the effects are limited to less than 0.02 eV. Even though low-energy sites can be found in layer B, there are also high-energy sites and high-energy barriers in between those within the GB layer, so the parallel diffusion does not take place within the GB layer, but rather involves excursion into the crystal grain and then trapping again within the GB.

In some cases, the diffusion of the H atom is accompanied by a change in the atomic arrangement of the Al

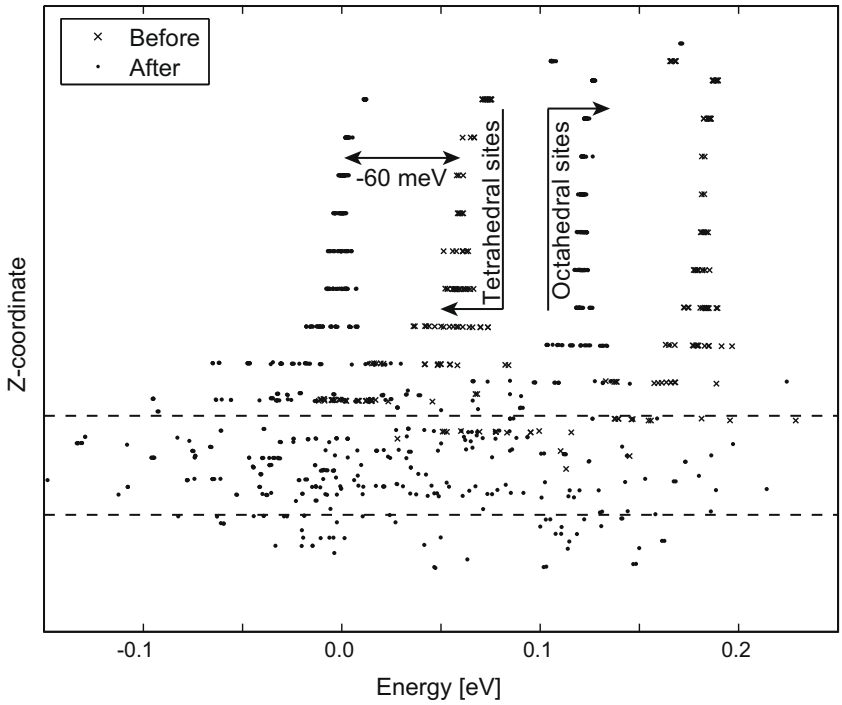

Fig. 6. Site energy as a function of the Z-coordinate of the H atom within the tilt GB. The dashed lines mark the GB region (defined as atoms that are not fcc-coordinated according to common neighbor analysis [18]). An annealing event that occurred during the simulation in iteration 250 shifted the site energy by −60 meV, hence the two peaks for both tetrahedral and octahedral sites, labelled "After" and "Before".

Table 6
Calculated diffusion constants.

	Crystal	Twist GB	Tilt GB	Twist + tilt GB
Diffusivity ($m^2\ s^{-1}$)	1.10×10^{-10}	1.26×10^{-10}	6.01×10^{-11}	3.47×10^{-12}

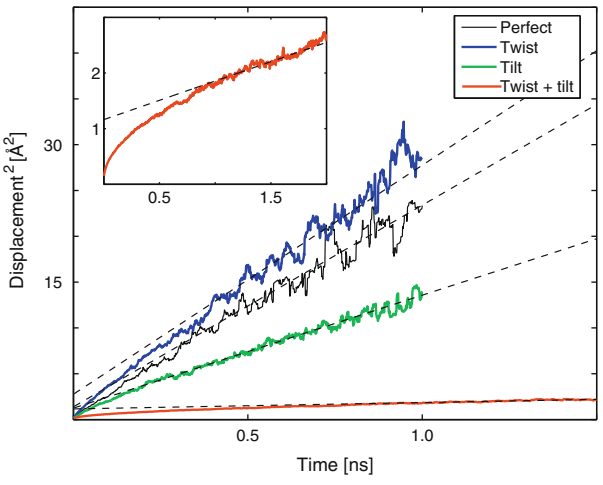

Fig. 7. Calculated 2D diffusivity parallel to the grain boundaries. The diffusion constants deduced from the curves are given in Table 6. When compared to a perfect crystal, the twist GB does not affect the parallel diffusivity strongly – a slight increase occurs. For the tilt GB the parallel diffusivity decreases by about half. The largest effect is seen for the twist + tilt GB, where the parallel diffusivity decreases by more than an order of magnitude compared to a perfect crystal.

atoms at the GB. One such event is shown in Fig. 11, where nine atoms are displaced by more than 0.5 Å in a transition involving a barrier of only 0.08 eV. The event took place in a region next to the GB layer, and the local structure changes from being (1 1 0) surface-like to being (1 1 1) surface-like. The Al atom labelled X residing at a (1 1 0) site in a neighboring layer gets pushed away from the rotational plane during the event, as (1 1 1) layers are separated by $\sqrt{6}/3$ in atomic distances, whereas the (1 1 0) layers are separated by 1/2.

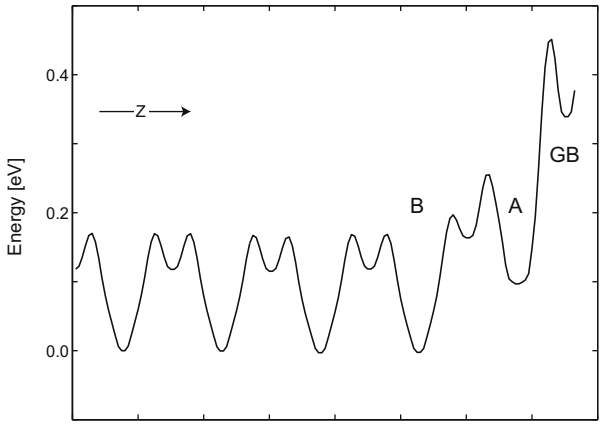

Fig. 8. Calculated minimum energy path for H atom diffusion perpendicular to the plane of a twist GB. The labelling is in accordance with Fig. 3. A striking feature is the large increase in energy close to the GB. This explains why the diffusion path does not cross the GB during the simulation.

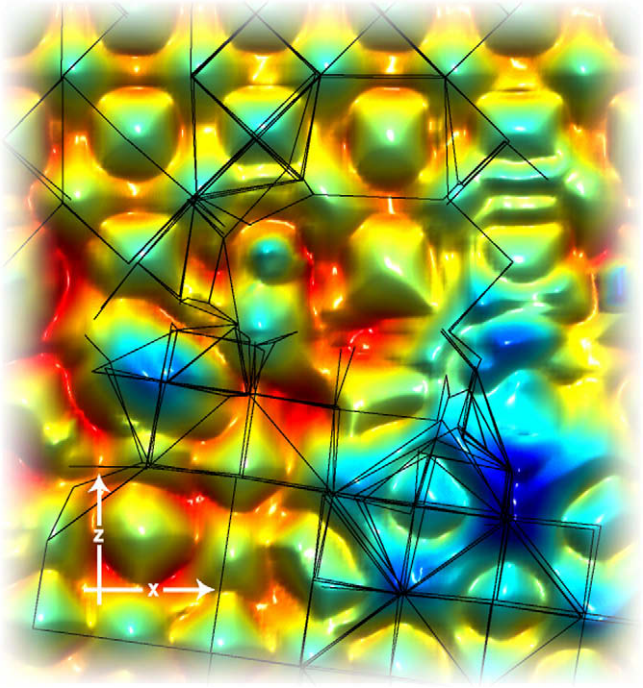

Fig. 9. Diffusion path overlayed on the calculated PES for a selected region near the tilt GB, as marked in Fig. 4. The PES is constructed from the lowest energy configurations in 10 equally separated parallel planes through the structure. From the PES it appears that there are two basins within the tilt GB which are irregular and have a high density of low-energy sites. The two basins correspond to the two channels observed in Fig. 4 interconnecting the upper and lower grain.

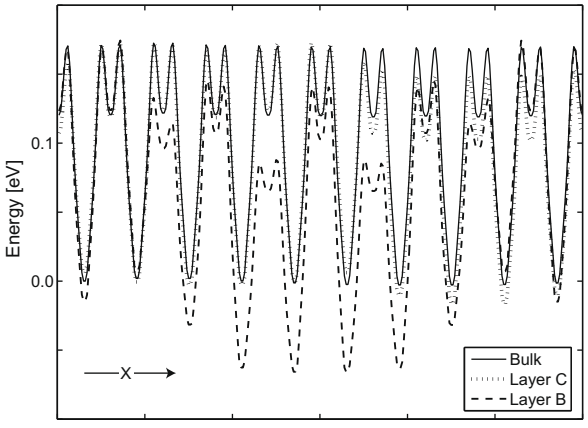

Fig. 10. Calculated minimum energy paths for H atom diffusion parallel to the plane of the tilt GB. The labelling is in accordance with Fig. 4. In layer B, the effective diffusion barrier has increased significantly, from 0.18 to 0.25 eV, as certain tetrahedral site configurations are lowered by 70 meV. From the minimum energy paths it appears that the effect of the tilt GB on diffusive behavior extends about three layers into the crystalline regions.

5.3. Twist + tilt grain boundary

The diffusivity at the twist + tilt GB is more than an order of magnitude smaller than in a perfect crystal. An inspection of the relevant minimum energy paths is more difficult here since the GB has more disorder. An analysis based on the energy of the sites visited during the simulation is shown in Fig. 12, where both the energy and the accumulated time are given as functions of the H atom's Z-coordinate. It is important to note that the time is not chronological time but, instead, a sum accumulated from all states visited where the Z-coordinate is smaller than the H atom's current value. From the plot it is evident that the H atom spends more than 99% of the total time in the GB region. About one-third of the time, the H atom is trapped in the region containing the six lowest energy sites, which are as much as 0.32 eV lower than the bulk sites. Clearly there is a large number of sites with low-energy in the GB region. The two groups of sites that stretch along the Z-coordinate axis represent the tetrahedral and octahedral sites, and their energy is clearly lowered when the GB is approached. A histogram of the energy of the sites is shown in Fig. 13. Apart from the peaks representing tetrahedral sites and octahedral sites, there is a broad distribution of low-energy sites within the GB layer, which can be represented by a Gaussian distribution to a reasonable approximation. This is in quite good qualitative agreement with experimental results on hydrogen in Pd [4].

From the large number of transitions that have been found during the simulation, one can check to see whether there is any correlation between activation energy and prefactor. A compensation effect where an increase in activation energy is accompanied by an increase in prefactor has been reported from experimental measurements [7]. The simulation data are shown in Fig. 14. Some compensation effect can be seen, but the effect is small.

6. Discussion

The main conclusion for the three inspected grain boundaries is that they do not significantly enhance hydrogen diffusion. Quite the opposite, in some cases they impede diffusion quite significantly. In the case of diffusion perpendicular to the Σ5 twist boundary, the diffusion is blocked by the grain boundary at room temperature. The tilt and twist + tilt grain boundaries cause trapping due to low-energy states within the boundary layer. Diffusion does not occur by hops between such trapping sites within the grain boundary layer, but rather when the hydrogen atom exits the grain boundary into one of the crystal grains. The twist boundary causes a slight increase in the diffusion parallel to the grain boundary, but this is mainly because of a confining effect that reduces the region the H atom can diffuse in, whereas the influence of the tilt and twist + tilt GB is a clear reduction, respectively by a half and by an order of magnitude of the value for a perfect crystal. In the case of the twist + tilt grain boundary the H atom trapping is so strong that the H atom ends up spending as much as 99% of the total simulated time in the grain boundary region.

Experiments on outgassing of hydrogen from cylindrical samples of aluminum of various grain sizes were carried out by Ichimura et al. [7]. They deduced a diffusion coefficient for hydrogen at low density as a function of grain diameter and observed a non-monotonic dependence: as

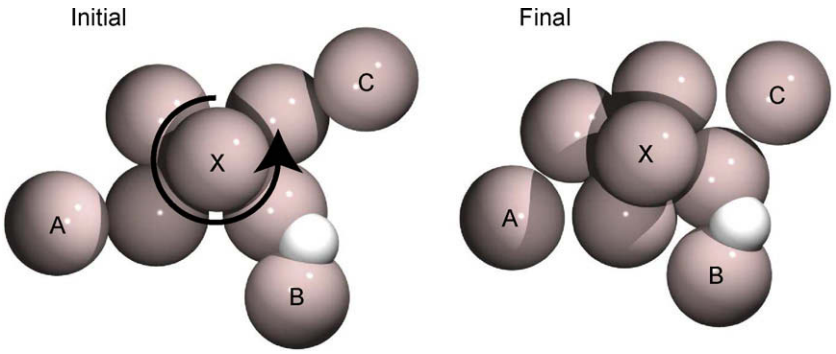

Fig. 11. Event taking place in a region next to the tilt GB where nine atoms get displaced by more than 0.5 Å in a concerted way. The labelled atoms are the ones mostly displaced. A, B and C can be assigned to the lower grain and X to the upper grain. The energy barrier is 80 meV. The local interface structure changes from being similar to a (1 1 0) surface to being similar to a (1 1 1) surface.

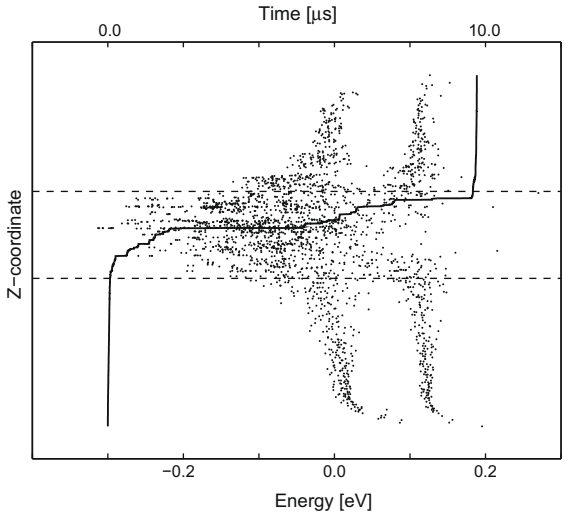

Fig. 12. The energy of sites and accumulated time from the simulation of H atom diffusion at the twist + tilt GB as functions of the Z-coordinate of the H atom. The zero of energy corresponds to a tetrahedral site in the crystal and the dashed lines mark the GB region as defined in Fig. 5. The main feature is that the H atom is confined in the GB region for more than 99% of the simulated time. This is consistent with the low parallel diffusivity shown in Fig. 7. The low-energy sites in the GB act as trapping sites for the H atom. The high density and wide scatter in energy for the stable states in the GB is in accordance with an experimentally deduced model [4].

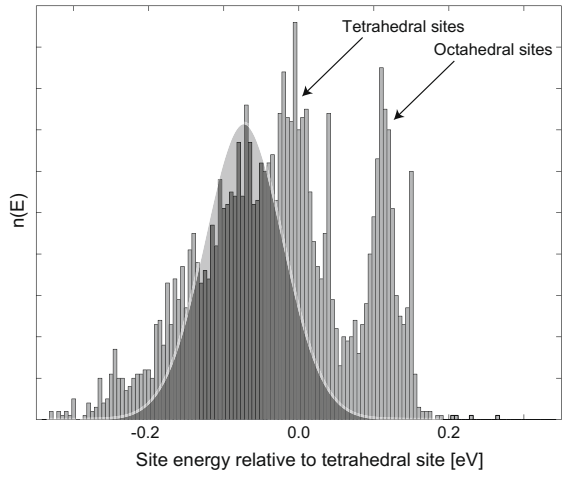

Fig. 13. Histogram of sites for the H atom in the twist + tilt GB. In addition to the peaks corresponding to tetrahedral sites and octahedral sites, there is a broad distribution of low-energy sites within the GB which can be approximated with a Guassian function, in qualitative agreement with the experimental results in Ref. [4].

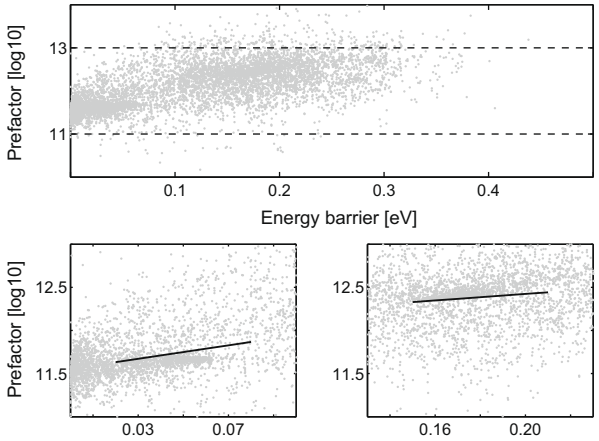

Fig. 14. Activation energy and prefactor for transitions that took place during the simulation of H atom diffusion near the twist + tilt GB. The uppermost figure includes all transitions. The bottom-left is a zoom on the low barrier region where, among other processes, the transitions from Oh to Th are include. The bottom-right figure is a zoom on the region that includes Th to Oh transitions. In both of the lower plots, the solid line is a linear fit. The positive slope of the lines indicates a weak compensation effect, especially in the low-energy region.

the grains were made smaller, a slight increase in diffusivity was observed for large, columnar grains, which was followed by a sharp decrease in diffusivity as the grains were made even smaller. Their interpretation of these results was that grain boundaries enhance diffusion, hence the initial increase in diffusion constant, but junctions of grain boundaries offer trapping sites that impede diffusion, hence the decrease in diffusion for smaller grains. Our simulation results offer an alternative explanation for these experimental results. The large, columnar grains will likely be surrounded by low-energy grain boundaries, such as the twist GB, and hydrogen atoms would be able to diffuse rapidly through the sample within a single grain and somewhat faster than in the crystal because of reflection from

the grain boundaries. In the smaller grains, which have a granular structure, the diffusion is impeded by grain boundaries, in particular higher curvature GBs, where trapping impedes diffusion. What effect trijunctions have on diffusion remains an interesting question. The simulation of atomic structure at trijunctions is more challenging than grain boundaries, but some progress has been made in that direction (see e.g. [19]), and hydrogen diffusion at trijunctions will be addressed in a future study.

It should be emphasized that the simulations only involve one H atom in the sample. Additional effects are expected when more than one hydrogen atom is present in the grain boundary, such as blocking of trapping sites and volume expansion when the hydride phase starts to form. The simulations are being extended to incorporate more hydrogen atoms to address these issues.

Acknowledgement

This work was funded by EC Integrated Project NESSHy and by the University of Iceland research fund.

References

[1] Edwards RAH, Eichenauer W. Scripta Metall 1980;14:971.
[2] Müetschele T, Kirchheim R. Scripta Metall 1987;21:1101.
[3] Young GA, Scully JR. Acta Mater 1998;46:6337.
[4] Müetschele T, Kirchheim R. Scripta Metall 1987;21:135.
[5] Harris TM, Latanision M. Metall Mater Trans A 1991;22:351.
[6] Yao J, Cahoom JR. Acta Metall Mater 1991;39:119.
[7] Ichimura M, Sasajima Y, Imabayashi M. Mater Trans JIM 1991;32(12):1109.
[8] Szpunar B, Lewis LJ, Swainson I, Erb U. Phys Rev B 1999;60:10107.
[9] Henkelman G, Jónsson H. J Chem Phys 2001;115(21):9657.
[10] Henkelman G, Jónsson H. Phys Rev Lett 2003;90(11):116101.
[11] Henkelman G, Jónsson H. J Chem Phys 1999;111(15):7010.
[12] Olsen RA, Kroes GJ, Henkelman G, Arnaldsson A, Jónsson H. J Chem Phys 2004;121:2004.
[13] Scully JR, Young GA, Smith SW. Mater Sci Forum 2000;331–337:1583.
[14] Wolverton C, Ozolic V, Asta M. Phys Rev B 2004;69:144109.
[15] Jacobsen KW, Stoltze P, Nørskov JK. Surf Sci 1996;366(2):394.
[16] Jacobsen KW, Nørskov JK, Puska MJ. Phys Rev B 1987;35(14):7423.
[17] Pedersen A, Henkelman G, Schiøtz J, Jónsson H. submitted for publication
[18] Clarke A, Jónsson H. Phys Rev E 1993;47:3975.
[19] Srinivasan SG, Cahn JW, Jónsson H, Kalonji G. Acta Mater 1999;47:2821.